

Kinetics of decomposition in ionic solids: III. Time evolution of phonons during spinodal decomposition in AgCl–NaCl

This article has been downloaded from IOPscience. Please scroll down to see the full text article.

2004 J. Phys.: Condens. Matter 16 5945

(<http://iopscience.iop.org/0953-8984/16/32/027>)

View [the table of contents for this issue](#), or go to the [journal homepage](#) for more

Download details:

IP Address: 129.252.86.83

The article was downloaded on 27/05/2010 at 16:42

Please note that [terms and conditions apply](#).

Kinetics of decomposition in ionic solids: III. Time evolution of phonons during spinodal decomposition in AgCl–NaCl

G Eckold¹, D Caspary¹, H Gibhardt¹, W Schmidt^{2,3} and A Hoser^{3,4}

¹ Institut für Physikalische Chemie, Universität Göttingen, Tammannstraße 6, D-37077 Göttingen, Germany

² Institut Laue-Langevin, 6 rue Jules Horowitz, BP 156, F-38042 Grenoble Cedex, France

³ Institut für Festkörperforschung, Forschungszentrum Jülich, D-52425 Jülich, Germany

⁴ Institut für Kristallographie, RWTH Aachen, D-52056 Aachen, Germany

Received 26 April 2004

Published 30 July 2004

Online at stacks.iop.org/JPhysCM/16/5945

doi:10.1088/0953-8984/16/32/027

Abstract

Real-time inelastic neutron scattering has been used to study the kinetics of the demixing process in AgCl–NaCl mixed single crystals. The variation of transverse acoustic phonon spectra provides the most direct information about the microscopic non-equilibrium behaviour. It is shown that a well defined splitting of phonon peaks corresponding to the formation of the product phases takes place on a timescale of seconds. Along with the observation of satellite reflections these findings clearly demonstrate that the phase separation is governed by the mechanism of spinodal decomposition in this ionic system. During the entire process the lattice parameter keeps almost unchanged, thus leading to a metastable state characterized by large coherency strains.

1. Introduction

Silver alkali halides provide interesting model systems for the study of decomposition processes in ionic solids. This is not only due to simple phase diagrams and the absence of structural phase transitions but also to the invariance of the anion sublattice, which is not involved in the demixing process. The phase separation is entirely confined to the cationic system and the anions provide an almost rigid frame. Along with the strong polarizability of silver ions, this feature guarantees that even single crystals are not destroyed during demixing [1]. Hence, the process of phase separation can be studied on a microscopic scale using lattice vibrations—phonons—as a local probe. In fact, time-resolved inelastic neutron scattering experiments are feasible even on a timescale of seconds using stroboscopic techniques [2]. This method provides the most direct information about the variation of interatomic interactions associated with the decomposition process.

Usually, demixing processes are studied by small angle scattering or by diffraction techniques. In the case of silver alkali halides, both yield, however, completely different time evolutions [3, 4]: within the spinodal regime, at temperatures well below the critical temperature T_c (198 °C in AgCl–NaCl [5]), the well known correlation peak at small angles corresponding to coherent concentration fluctuations [6–10] appears on a timescale of seconds. In contrast, the splitting of Bragg reflections due to the different lattice parameters of the product phases is observed only after much longer time intervals which are of the order of years at room temperature. From these investigations, it was concluded that chemical demixing and the relaxation of the lattice are two different aspects of the phase separation.

As shown in a static phonon study on AgCl–NaCl mixed crystals [11], the product phases exhibit readily distinguishable phonon spectra. In particular, the transverse acoustic phonons are well separated due to the different elastic constants of AgCl and NaCl. In this paper, we present the results of time-resolved phonon investigations that directly reflect the change of interatomic forces during demixing. By comparison with the time evolution of Bragg reflections, it will be demonstrated that the phase separation is, in fact, independent of the lattice relaxation.

2. Experimental details

Large (cm^3) single crystals of $\text{Ag}_x\text{Na}_{1-x}\text{Cl}$ with different compositions x were grown from the melt by the Czochralski method. Details are presented elsewhere [11, 12]. For the present experiments, crystals with AgCl concentrations of $x = 0.41$ (crystal A), 0.26 (crystal B) and 0.23 (crystal C) were used. Their quality was checked by gamma-ray diffraction yielding mosaicities of less than 1° .

Specially designed furnaces were developed which were optimized for rapid cooling and heating in normal atmosphere. Details may be found in [12]. The crystals were wrapped in silver foil in order to guarantee the temperature homogeneity.

The neutron scattering experiments were performed at the three-axis spectrometer IN12 (HFR, ILL-Grenoble) using different combinations of neutron energy, collimation etc. For the time-resolved investigations, a portable data acquisition system was developed that can be used with different spectrometers and is described in some detail in [13]. During the experiments the sample was periodically heated to the homogenization temperature of about 400 °C and quenched to the decomposition temperature of 100 °C. The quench rate was about $5\text{--}7 \text{ K s}^{-1}$. The cycle period was 600 s and the neutrons were counted in time channels of 10 s. In order to improve the statistics the raw data were, in general, averaged over three time channels. Most of the data were obtained observing the transverse acoustic phonon along $(\xi 00)$ at $\xi = 0.3$. For comparison, the evolution of the (200) Bragg reflection was determined on the same timescale.

Additional experiments were performed on the three-axis spectrometer UNIDAS (FRJ-2, Jülich) on a longer timescale and with lower quench rates.

3. Results and discussion

3.1. Evolution of phonon spectra

Figure 1 shows the time evolution of transverse acoustic phonon spectra for two different concentrations at $q = (0.3 \ 0 \ 0)$ after quenching to $T = 100^\circ\text{C}$, which is about 100 K below T_c . The time zero is defined as the instant when the miscibility gap is entered. The final temperature was reached after about 23 s. The phonon of the homogeneous phase is centred at 0.73 THz for crystal A ($x = 0.41$) and at 0.92 THz for crystal C ($x = 0.23$), respectively.

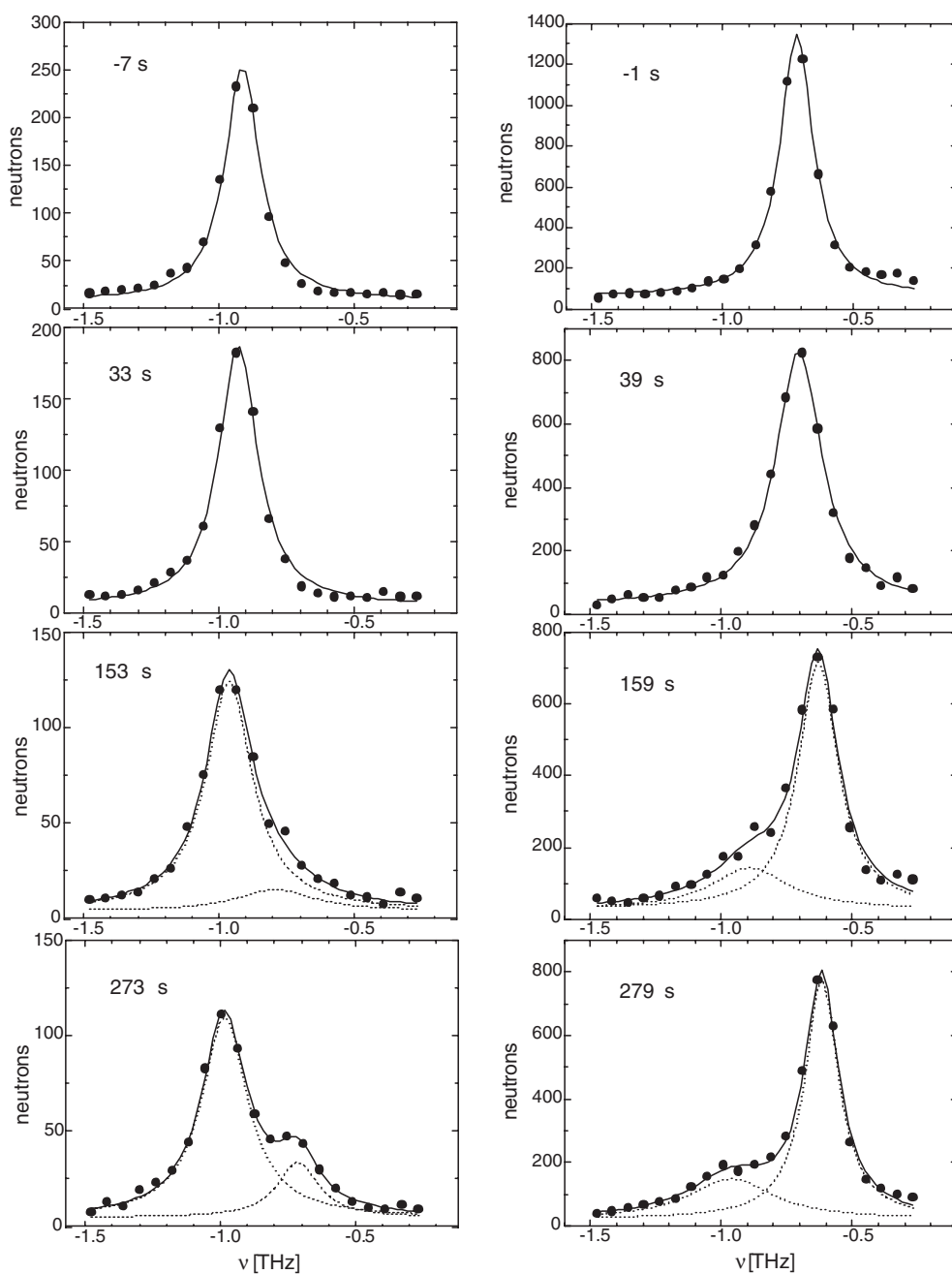


Figure 1. Time evolution of transverse acoustic phonons at $q = (0.3\ 0\ 0)$ in crystal C ($x = 0.23$) (left) and crystal A ($x = 0.41$) (right) at 100°C .

During cooling, the intensity of the phonon peak decreases according to the Bose factor. On a timescale of some 10 s, the phonon splits into two well defined components corresponding to the two product phases. The individual spectra can well be fitted to the sum of two Lorentzians. The silver rich phase is represented by the phonon at lower frequencies while the sodium

rich phase with its larger elastic constant c_{44} corresponds to the phonon close to 1 THz. The intensities of the acoustic phonons are determined by the volume fractions of the corresponding phases and the different dynamical structure factors which are inversely proportional to the square of the phonon frequencies. Neglecting the difference in the temperature factors, the intensity ratio can be written as

$$\frac{I_1}{I_2} = \frac{V_1}{V_2} \left(\frac{F_1}{F_2} \right)^2 \left(\frac{\nu_2}{\nu_1} \right)^2 \quad (1)$$

where the F_i are the scattering lengths of the two phases

$$F_i = b_{\text{Cl}} + x_i b_{\text{Ag}} + (1 - x_i) b_{\text{Na}} \quad (2)$$

and V_i and ν_i are the corresponding volumes and frequencies, respectively.

The time-dependences of the phonon frequencies and intensities are shown in figure 2 for crystal A. It is easily seen that the phase separation takes place within seconds and changes the interatomic forces that determine the phonon frequencies. After about 80 s, the splitting into two components is almost completed and the intensities keep constant.

3.2. Elastic satellite reflections

At the same time, the position of Bragg reflections and, hence, the lattice parameter remains almost unchanged. Consequently, the crystal adopts a metastable state that is associated with large coherency strains. It was demonstrated in a previous paper about experiments on polycrystalline samples that the lattice relaxation and the release of those strains take place on a much longer timescale [4]. This finding is confirmed by the present time-resolved experiments on single crystals. Due to the better resolution in Q -space, however, an additional feature is observed as shown in figure 3: close to the Bragg peaks satellites appear that correspond to the modulation of concentration. These satellites cannot be mistaken for the Bragg peaks that are expected for the product phases in equilibrium since, as a function of time, the peak positions shift towards the central Bragg reflection as illustrated by the inset of figure 3. Initially, the satellites are even found well beyond the Bragg positions of the pure compounds AgCl and NaCl. At long times, the time evolution can be described by the Lifshitz–Slyozov $t^{-1/3}$ -law [14] and after several thousand seconds the side peaks merge with the fundamental Bragg reflection. This finding is in very good agreement with the results of neutron small angle scattering on powder specimens that revealed a time-dependent correlation peak with almost the same wavevector [4]. Moreover, the satellites have not only been observed for crystal A but also for crystal C with a different overall composition. In both cases, the peak positions are almost identical. Hence, the appearance of these satellites provides additional strong evidence for the existence of a correlated concentration wave that is a characteristic feature of spinodal decomposition.

The satellites are observed in longitudinal scans along the [100]-direction. No attempt has, however, been made so far to determine the direction of the satellite wavevector precisely. The experimental resolution as well as the mosaicity of the crystal did not allow us to extract this information from the present experiments.

From the satellite position a characteristic correlation length of the order of 20–30 nm is obtained after 1000 s. This is considerably larger than the coherence length of a typical phonon, which may be estimated from the heat conductivity to be of the order of 2–5 nm. Coarsening effects usually go hand in hand with the squaring of the modulation wave. Consequently, the system may be regarded as an arrangement of microdomains. For a system of almost critical concentration (like crystal A), these domains exhibit similar volumes and, hence, the phonon spectra are essentially determined by the superposition of well defined phonons of the individual phases. Thus, the phonons probe the local concentrations. For off-critical systems

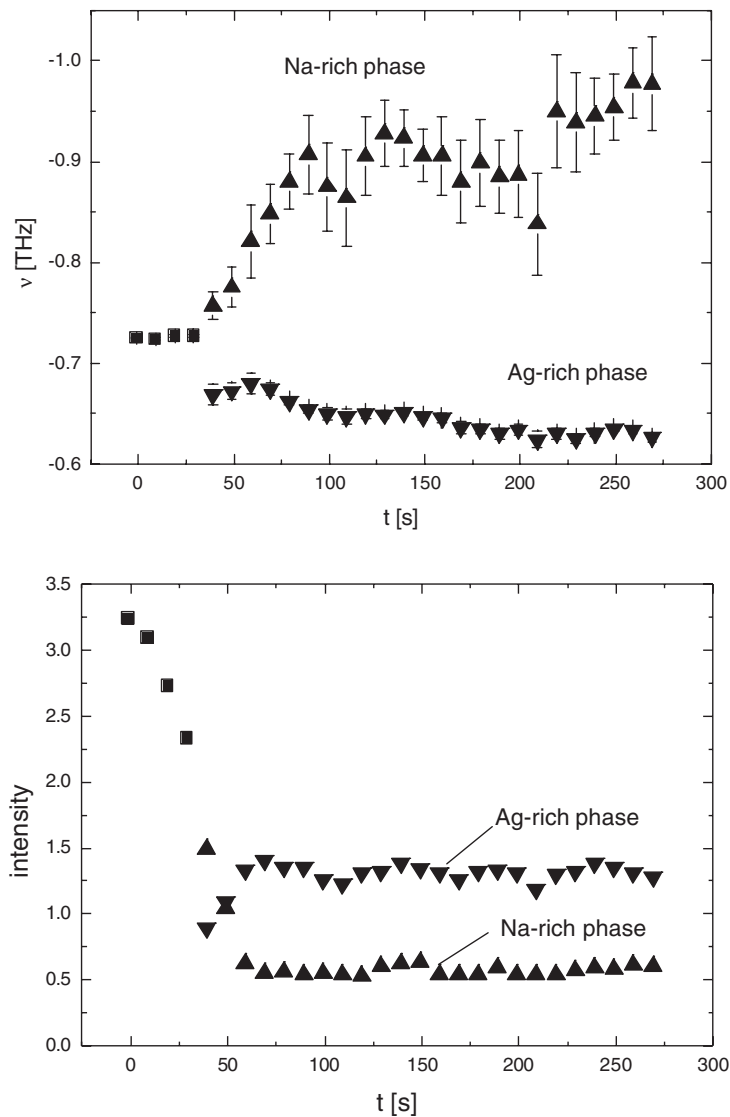


Figure 2. Time evolution of the frequencies (top) and the integrated intensities (bottom) for the TA (0.3 0 0) phonons in $\text{Ag}_{0.41}\text{Na}_{0.59}\text{Cl}$ at 100°C .

(like crystal C), however, the characteristic size of the minority phase becomes comparable to the coherence length of the phonons. In this case, interface effects are no longer negligible and the corresponding phonons are determined by some average of the interatomic forces within both domains.

3.3. Determination of local concentrations

If we use the frequency–concentration diagram as determined previously from equilibrium experiments in the homogeneous phase at 330°C [11] and take into account the temperature dependence of the phonon frequencies via the temperature coefficients of c_{44} [15], we can tentatively assign local concentrations to the two phases.

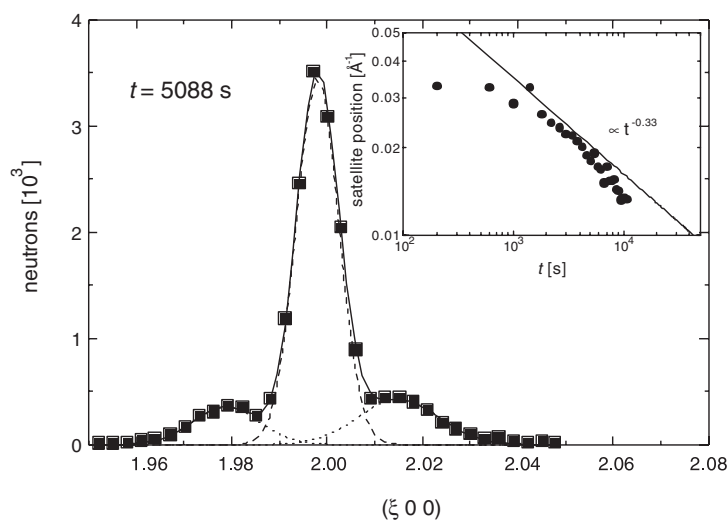


Figure 3. Elastic satellites close to the (2 0 0) Bragg reflexion. The inset shows the time dependence of the satellite position.

After 300 s, the sodium-rich phase exhibits a phonon frequency of about 0.98 THz for both crystals A and C as shown in figure 2. This value corresponds to a concentration of $x_1 \approx 0.20$.

At the same time, the frequency of the silver-rich phase depends on the overall composition of the sample. While in crystal A ($x = 0.41$) the phonon is observed at 0.62 THz, it appears at the considerably larger frequency of 0.72 THz in the sodium-rich crystal C ($x = 0.23$). The latter contains only small silver-rich domains and the phonon is not completely determined by the respective concentration. Therefore, we use the data of crystal A to determine the concentration of the silver-rich domain as $x_2 \approx 0.60$. Owing to the fact that the phonon frequency is only weakly concentration dependent in the silver-rich regime [11] this value should merely be regarded as a rough estimate.

On the basis of these concentrations, the volume fraction of the silver-rich phase can be calculated from the lever rule to be 0.53 for crystal A. These data are in excellent agreement with the intensity ratio of the phonons according to equation (1), thus proving the consistency of the present interpretation of the data.

The concentrations correspond to the metastable, coherent miscibility gap that is different from the equilibrium miscibility gap (binodal) due to the existence of coherency strains originating from the different lattice parameters of the constituents. It has been shown in [4] that the coherent critical point is suppressed with respect to the incoherent one by about 20 °C in very good agreement with estimations from the lattice parameter mismatch (1.7%) and the average Young modulus (30.2 GPa) according to Cahn [16]. At 100 °C, the width of the coherent miscibility gap is obtained from the present phonon data as $\Delta x = x_2 - x_1 \approx 0.40$. In spite of the fact that x_2 cannot be determined very precisely, there is a remarkable agreement with the findings from small angle scattering [4] that yield $\Delta x \approx 0.46$. Note that the small angle intensity is essentially determined by the concentration difference rather than the individual concentrations. The phase diagram shown in [4] is therefore based on the assumption that the binodal as well as the metastable, coherent miscibility gap is symmetric with respect to $x = 0.5$. The present results from inelastic scattering indicate, however, that the coherent gap might be asymmetric in shape, as illustrated schematically in figure 4. The temperature shift

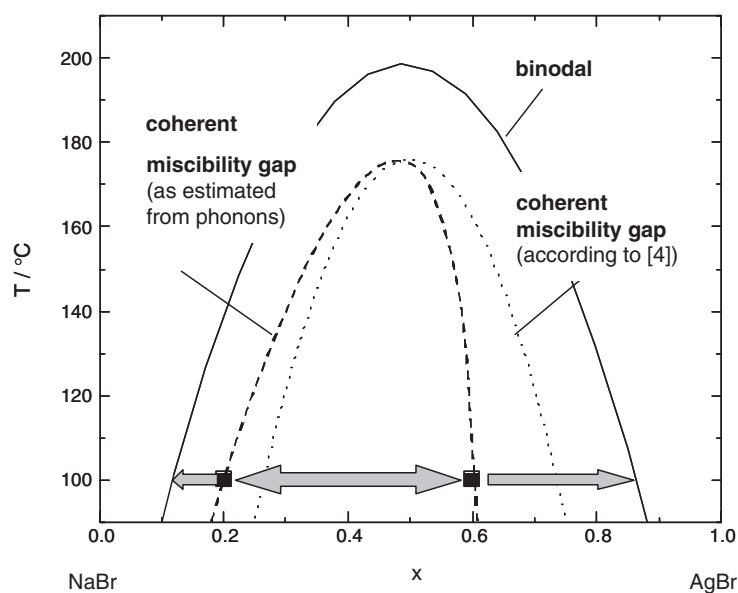


Figure 4. Schematic representation of the phase diagram: the binodal is based on equilibrium data of Sinistri *et al* [5]. The dotted curve corresponds to the symmetric coherent miscibility gap as deduced from small angle scattering [4] while the dashed curve is the estimated asymmetric metastable gap taking into account the results of the present phonon investigation (■). The double arrow represents the first stage of decomposition that leads to concentrations on the metastable gap, while the outer arrows illustrate the final equilibration.

with respect to the binodal curve seems to be more pronounced in the silver-rich part of the phase diagram. This finding is not unexpected since the elastic stiffness of AgCl is about 50% larger than that of NaCl [15]. Hence, there is a considerable asymmetry of the elastic properties and a stronger suppression of the coherent miscibility gap in the silver-rich regime seems likely.

In the sodium-rich crystal C, the typical domain size of the minority phase can be calculated from the correlation length d as determined by the satellite reflections. Assuming that these domains are small spheres of radius r embedded statistically within the remaining crystal, the volume fraction is given by

$$\frac{V_{\text{minority}}}{V_{\text{total}}} = \frac{4\pi}{3} \frac{r^3}{d^3}. \quad (3)$$

Inspection of figure 3 yields a correlation length of 20 nm after 300 s and thus, along with the volume fraction of 0.08, a characteristic domain size of the minority phase of $r \approx 5$ nm results. This value is comparable to the phonon coherence length. Hence, phonons are likely to travel across the domain boundary thus averaging over a larger volume. Consequently, they exhibit an increased intensity and an average frequency of about 0.72 THz which is considerably larger than that of the silver-rich phase (see figure 1). Only if the demixing process proceeds towards larger structures will the true property of the minority phase become visible.

3.4. Phonon line-widths

The phonon line-widths are of particular interest since they may provide information about the damping of lattice vibrations in inhomogeneous systems. Due to the limited counting statistics, the present results do not allow us, however, to determine the line-widths very accurately. The

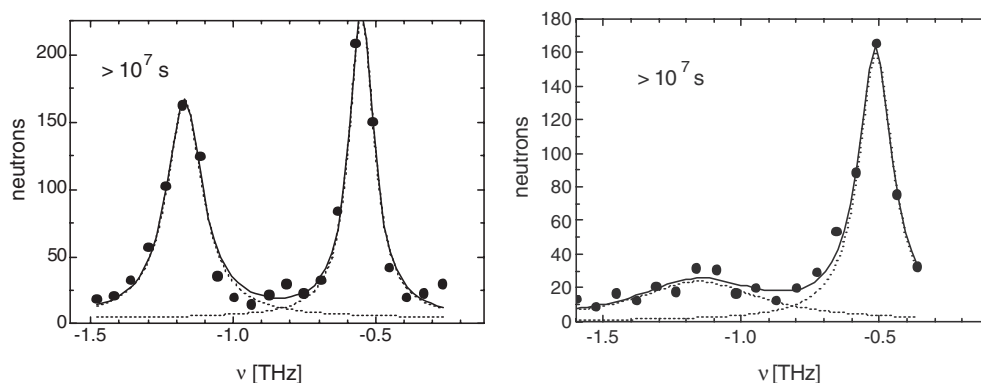


Figure 5. Spectra of the transverse acoustic phonon at $q = (0.3\ 0\ 0)$ after ageing for several months at ambient temperature for crystal C ($x = 0.23$) (left) and crystal A ($x = 0.41$) (right).

most that can be said for crystal A ($x = 0.41$) is that the phonon of the silver-rich phase is essentially determined by the experimental resolution while that of the sodium-rich phase is considerably broader, with an intrinsic line-width of the order of 0.25 THz (as obtained after deconvolution with the resolution function). In view of the lower Debye temperature of AgCl, anharmonic effects are unlikely to account for this difference since these should lead to the opposite effect. Instead, concentration gradients as the characteristic features of spinodal decomposition are believed to be responsible for the substantial broadening of the high frequency phonon. In fact, a variation of the mole fraction by $\Delta x = 0.2$ leads to frequency shifts of about 0.25 THz in sodium-rich crystals but of only a few 0.01 THz in silver-rich crystals [11].

3.5. Long-time behaviour

The phonon spectra obtained after about 300 s are different from those that are observed in (quasi-)equilibrium after several months of demixing [11]. In figure 5, spectra that have been obtained after a very long time of decomposition at room temperature are shown. (Note that the temperature shift of phonon frequencies can be estimated from the temperature coefficients of the elastic constants [15] to be of the order of 0.01 THz between room temperature and 100 °C and is thus of minor importance for the present discussion.) Obviously, there is a significant shift of phonon frequencies and intensities on a timescale of months. It should be noted that the intensity change is essentially due to the $1/\nu^2$ -factor in the dynamical structure factor (equation (1)) rather than to a variation of the volume fractions of the corresponding phases.

Additional long-time experiments on crystal B with $x = 0.26$ (see figure 6) reveal that even after 2×10^4 s the phonons are considerably different from those observed in the final state. Note that these data have been obtained under somewhat different quenching conditions. Hence, the initial splitting is somewhat delayed as compared to the data of figures 1 and 2.

The long-time relaxation seems to be associated with shifts of concentrations from the spinodal up to the binodal as illustrated in figure 4. Moreover, the Bragg peaks start to separate into two components of different lattice parameters, thus indicating the release of mechanical strains.

The effect of internal strains or stresses on the phonon frequencies can be estimated from the pressure coefficients of the elastic constant c_{44} . Interestingly, different to NaCl ($\frac{1}{c_{44}} \frac{\partial c_{44}}{\partial p} \Big|_{\text{NaCl}} = 29 \times 10^{-12} \text{ Pa}^{-1}$) AgCl exhibits a negative coefficient ($\frac{1}{c_{44}} \frac{\partial c_{44}}{\partial p} \Big|_{\text{AgCl}} =$

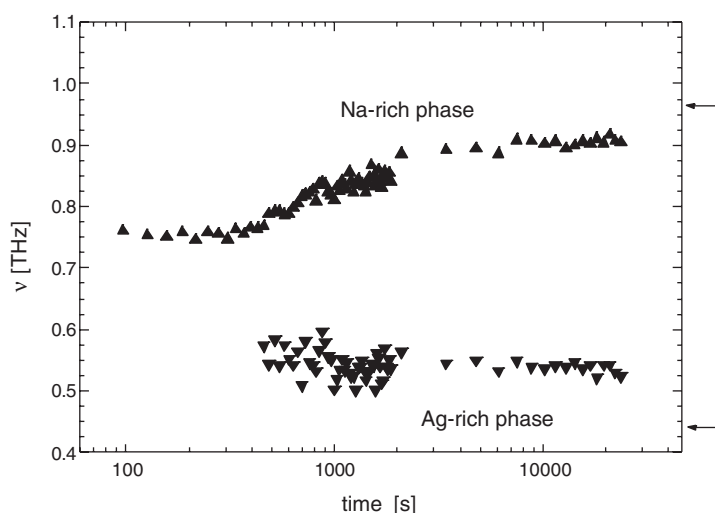


Figure 6. Long-time behaviour of the frequencies for the TA (0.25 0 0) phonon in crystal B ($x = 0.26$) on a logarithmic scale. The arrows indicate the limiting frequencies observed after several months. (Note that the initial splitting is somewhat delayed due to smaller quench rate.)

$-81.2 \times 10^{-12} \text{ Pa}^{-1}$) [15]. During demixing, the sodium- (silver-) rich phase exists with a smaller (larger) lattice parameter as compared to the equilibrium value. Hence, it is subjected to compressive (tensile) stresses of the order of -350 (650) MPa. The release of these stresses would lead to an additional phonon frequency shift of only -0.5% and 2.6% . Hence, it is concluded that the dominating dynamical long-time effect is, in fact, due to the shift of concentrations towards the equilibrium values located on the binodal.

4. Conclusion

The time evolution of phonon spectra was observed in mixed single crystals of AgCl and NaCl after quenching into the miscibility gap. It could be shown that the lattice vibrations, as fingerprints of the local interatomic forces, change immediately on a timescale of seconds or minutes. The splitting of a single phonon into two well defined components clearly demonstrates the chemical demixing even if the lattice parameter remains almost unchanged. Obviously, the lattice is conserved by the almost rigid anion sublattice that is not affected by the demixing process. Hence, the crystal enters a metastable state that is characterized by internal stresses of several hundred MPa. The present findings provide clear evidence for the mechanism of spinodal decomposition which may be described by three stages.

In the first stage, demixing leads to two phases with concentrations on the metastable, coherent miscibility gap. The phonon data indicate that this coherent gap is not symmetric around $x = 0.5$ but considerably steeper in the silver-rich regime of the phase diagram. At short times of the order of 10–100 s, concentration fluctuations with a characteristic wavelength of the order 20 nm dominate the phase separation and lead to a periodic decomposition pattern. This is reflected by satellite peaks close to Bragg reflections as well as by the correlation peak at small angles.

The second stage on a timescale of minutes or hours is characterized by the coarsening of the domain pattern and associated with a gradual shift of the satellites (and the correlation peak) to smaller wavevectors.

The mechanical relaxation of the lattice occurs on a much longer timescale of months. This final stage is associated with the release of mechanical strains as well as a gradual shift of concentrations from the coherent miscibility gap to the binodal. The splitting of Bragg reflections and the shift of phonons towards the equilibrium positions are characteristic features of the long-time behaviour.

References

- [1] Windgasse J, Eckold G and Güthoff F 1997 *Physica B* **234–236** 153
- [2] Elter P, Eckold G, Caspary D, Güthoff F and Hoser A 2002 *Appl. Phys. A* **74** S1179
- [3] Eckold G 2001 *J. Phys.: Condens. Matter* **13** 217
- [4] Caspary D, Eckold G, Güthoff F and Pyckhout-Hintzen W 2001 *J. Phys.: Condens. Matter* **13** 11521
- [5] Sinistri C, Riccardi R, Margheritis C and Tittarelli P 1971 *Z. Naturf. a* **27** 149
- [6] Binder K and Stauffer D 1974 *Phys. Rev. Lett.* **33** 1006
- [7] Binder K, Billotet C and Mirolid P 1978 *Z. Phys.* **1330** 183
- [8] Furukawa H 1981 *Phys. Rev. A* **23** 1535
- [9] Binder K and Heermann D W 1985 *Scaling Phenomena in Disordered Systems* ed R Pynn and A Skjeltrop (New York: Plenum) p 207
- [10] Heermann D W and Binder K 1987 *The Physics of Structure Formation* ed W Güttinger and G Dangelmayr (Berlin: Springer) p 42
- [11] Caspary D, Eckold G, Elter P, Gibhardt H, Güthoff F, Demmel F, Hoser A, Schmidt W and Schweika W 2003 *J. Phys.: Condens. Matter* **15** 6415
- [12] Caspary D 2003 *Thesis* University of Göttingen
- [13] Eckold G, Gibhardt H, Caspary D, Elter P and Elisbihani K 2003 *Z. Kristallogr.* **218** 154
- [14] Lifshitz I M and Slyozov V V 1961 *J. Phys. Chem. Solids* **19** 35
- [15] Every A G and McCurdy A K 1992 *Landolt–Börnstein New Series* vol 29, ed D F Nelson (Berlin: Springer) p 76, 77, 240
- [16] Cahn J W 1961 *Acta Metall.* **9** 795